A fast simulation method for 1D heat conduction

Automation and Control Institute (ACIN)
Vienna University of Technology
Gusshausstrasse 27-29/E376
1040 Vienna, Austria

Internet: www.acin.tuwien.ac.at
E-mail: office@acin.tuwien.ac.at
Phone: +43 1 58801 37601
Fax: +43 1 58801 37699

A fast simulation method for 1D heat conduction☆

A. Steinboeck*[a], D. Wild[b], T. Kiefer[b], A. Kugi[a]

[a]*Automation and Control Institute, Vienna University of Technology, Gusshausstrasse 27–29, 1040 Wien, Austria*
[b]*AG der Dillinger Hüttenwerke, Werkstrasse 1, 66763 Dillingen/Saar, Germany*

Abstract

A flexible solution method for the initial-boundary value problem of the temperature field in a one-dimensional domain of a solid with significantly nonlinear material parameters and radiation boundary conditions is proposed. A transformation of the temperature values allows to isolate the nonlinear material characteristics into a single coefficient of the heat conduction equation. The Galerkin method is utilized for spatial discretization of the problem and integration of the time domain is done by constraining the boundary heat fluxes to piecewise linear, discontinuous signals. The radiative heat exchange is computed with the help of the Stefan-Boltzmann law, such that the ambient temperatures serve as system inputs. The feasibility and accuracy of the proposed method are demonstrated by means of an example of heat treatment of a steel slab, where numerical results are compared to the finite difference method.

Key words: heat conduction, nonlinear material parameters, method of weighted residuals, Galerkin method, radiative heat exchange, implicit difference equation

1. Introduction

In process control applications, there is a need for mathematical models which are both computationally inexpensive as well as reliable in terms of accuracy and convergence. These requirements are particularly important for models to be used in real-time applications like trajectory planning, optimization, or control. Motivated by these needs, a method to determine the transient temperature field in a one-dimensional domain of a solid with significantly nonlinear material parameters and radiation boundary conditions is proposed. The approach originates from an application in the steel industry, where slabs or rolled products are to be heat-treated or reheated according to specific temperature trajectories [2, 21, 22]. However, by analogy, the method can be applied to other diffusion-convection systems described by parabolic initial-boundary value problems.

The paper is organized as follows: Section 2 starts with a brief review of the heat conduction equation (strong formulation) with nonlinear material parameters and Neumann boundary conditions, followed by a transformation of the temperature such that the nonlinearity is isolated into a single parameter of the parabolic problem. Thereupon, the problem is restated in the weak formulation, which is suitable for the Method of Weighted Residuals (MWR). Here, the Galerkin Method (GM) is employed to derive a low-dimensional lumped-parameter system, and a time integration method is proposed which allows for piecewise linear, discontinuous input signals. Finally, the boundary conditions are supplemented by elementary laws of thermal radiation. The feasibility and the accuracy of the proposed method are examined by means of an example of heat treatment of a steel slab in Section 3. For comparison, also the Finite Difference Method (FDM) is applied to the problem under consideration. A brief overview of the assumptions and approximations utilized in this work is given in the final Section 4.

☆A preliminary version of this paper was presented at the 6th Vienna Conference on Mathematical Modelling in February 2009, cf. [20].

*Corresponding author.
Email address: andreas.steinboeck@tuwien.ac.at (A. Steinboeck)

Post-print version of the article: A. Steinboeck, D. Wild, T. Kiefer, and A. Kugi, "A fast simulation method for 1D heat conduction", *Mathematics and Computers in Simulation*, vol. 82, no. 3, pp. 392–403, 2011. DOI: 10.1016/j.matcom.2010.10.016
The content of this post-print version is identical to the published paper but without the publisher's final layout or copy editing.

2. Theoretical concept

2.1. Heat conduction problem with Neumann boundary conditions

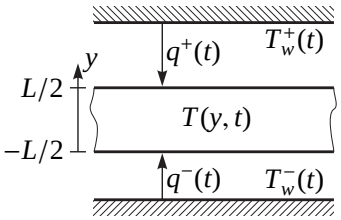

Figure 1: An infinitely extended solid with radiation boundary conditions.

Let $T(y,t)$ be the temperature field in a solid defined along the spatial dimension y with $y \in [-L/2, L/2]$, as shown in Fig. 1. Here, y is a Lagrangian coordinate, and the absolute temperature T is considered constant along any direction orthogonal to y. The heat flux $q(y,t)$ inside the solid is determined by the properties of the material, the temperature gradient, and the boundary conditions at $y = \mp L/2$. In this analysis, neither heat sources nor heat sinks inside the solid are considered.

Fourier's law is defined as $q(y,t) = -\lambda \partial T(y,t)/\partial y$, with the thermal conductivity λ. Therefore, the heat conduction process can be defined by the diffusion law [1, 12]

$$\rho c \frac{\partial T(y,t)}{\partial t} = -\frac{\partial q(y,t)}{\partial y} = \frac{\partial}{\partial y}\left(\lambda \frac{\partial T(y,t)}{\partial y}\right) \qquad y \in (-L/2, L/2)\,,\ t > 0 \tag{1a}$$

with initial conditions

$$T(y,0) = T_0(y) \qquad y \in [-L/2, L/2] \tag{1b}$$

and Neumann boundary conditions

$$q(\mp L/2, t) = -\lambda \left.\frac{\partial T(y,t)}{\partial y}\right|_{y=\mp L/2} = \pm q^{\mp}(t) \qquad t > 0. \tag{1c}$$

The heat inputs $q^-(t)$ and $q^+(t)$ define the heat exchange between the solid and its environment, as indicated in Fig. 1. They may depend on the surface temperatures $T(-L/2,t)$ and $T(L/2,t)$, respectively. Here, the heat conduction problem is given in its *strong* formulation. Section 2.3 touches upon the corresponding *weak* formulation and its solution by means of the MWR.

In (1), ρ represents the mass density, which may depend on y only. The specific heat capacity c and the thermal conductivity λ may depend on y or T or both. However, in this analysis, a homogeneous material, i. e. independence of the parameters from y, is stipulated. Moreover, possible dependence of the parameters on the history of T is disregarded, i. e. c and λ may only depend on the current local temperature. The nonlinear temperature dependence of c and λ renders the partial differential equation (1) nonlinear.

An example for the dependence of the parameters on the local temperature $T(y,t)$ is given in Fig. 2 for standard steel (0.1 % carbon). The salient peak of c corresponds to a phase transition. Throughout this analysis, if temperature dependence is accounted for, data from Fig. 2 is used. More information on the temperature dependence of material parameters may be obtained from [4, 10].

2.2. Transformation of temperature

If the MWR were applied directly to (1), generally an *implicit* differential algebraic equation would be obtained. Fortunately, a simple transformation of the temperature allows to isolate the nonlinear material characteristics into a *single* parameter, as demonstrated in [1] by elimination of the temperature dependence of λ. In an analogous way, the

Post-print version of the article: A. Steinboeck, D. Wild, T. Kiefer, and A. Kugi, "A fast simulation method for 1D heat conduction", *Mathematics and Computers in Simulation*, vol. 82, no. 3, pp. 392–403, 2011. DOI: 10.1016/j.matcom.2010.10.016
The content of this post-print version is identical to the published paper but without the publisher's final layout or copy editing.

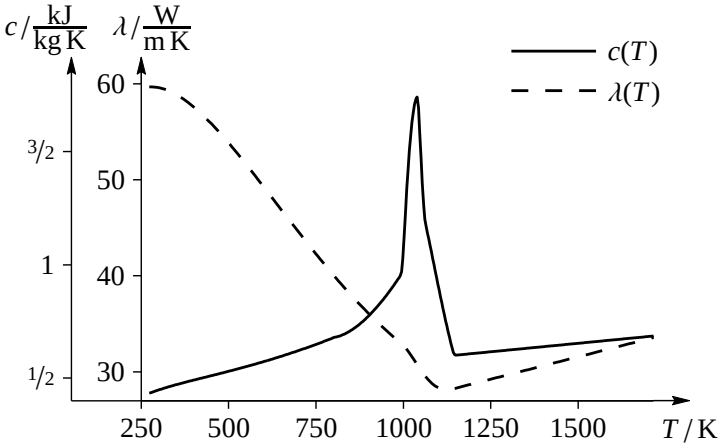

Figure 2: Temperature dependent material parameters for standard steel with 0.1 % carbon (data adapted from [10]).

temperature dependence of c is eliminated in the sequel, such that the MWR will finally furnish an *explicit* Ordinary Differential Equation (ODE). The transformation law reads as

$$\tilde{T}(T) := \tilde{T}_0 + \frac{1}{\tilde{c}} \int_{\bar{T}_0}^{T} c(\tau)\mathrm{d}\tau. \tag{2}$$

It is generally *nonlinear* and *time-invariant*. Bijectivity of the transformation is ensured if $c(T) > 0 \; \forall \, T$—a condition that is satisfied for all practical purposes. Generally, an analytical expression for the inverse transformation $T(\tilde{T})$ cannot be given, however, a simple look-up table will be sufficient for computer implementations. The transformed state $\tilde{T}$ is proportional to the specific enthalpy, with the proportionality coefficient $1/\tilde{c}$. The *constant* parameters $\tilde{T}_0$, $\bar{T}_0$, and $\tilde{c}$ may be chosen at will. However, the stipulations $\bar{T}_0 = \tilde{T}_0$ and $\tilde{c} = c(\bar{T}_0)$ seem reasonable and will be used hereinafter. Thus, the slope of $T(\tilde{T})$ at $\tilde{T} = \tilde{T}_0$ is 1. If c is constant, (2) simplifies to the identity function.

Utilization of (2) and introduction of the differential operators

$$\mathcal{D}(\tilde{T}) := \rho\tilde{c}\frac{\partial \tilde{T}}{\partial t} - \frac{\partial}{\partial y}\Bigg(\underbrace{\lambda(T(\tilde{T}))\frac{\tilde{c}}{c(T(\tilde{T}))}}_{=:\,\tilde{\lambda}(\tilde{T})} \frac{\partial \tilde{T}}{\partial y} \Bigg)$$

$$\mathcal{B}^{\mp}(\tilde{T}) := -q^{\mp}(t) \mp \tilde{\lambda}\, \frac{\partial \tilde{T}}{\partial y}\bigg|_{y=\mp L/2}$$

allow to reformulate (1) as

$$\mathcal{D}(\tilde{T}(y,t)) = 0 \qquad y \in (-L/2, L/2)\,, \; t > 0 \tag{3a}$$

with initial condition (1b) and Neumann boundary conditions

$$\mathcal{B}^{-}(\tilde{T}(y,t)) = \mathcal{B}^{+}(\tilde{T}(y,t)) = 0 \qquad t > 0. \tag{3b}$$

It is assumed that $\tilde{T}(y,t)$ always satisfies the differentiability requirements induced by the operators $\mathcal{D}$ and $\mathcal{B}^{\mp}$. Obviously, $q(y,t) = -\tilde{\lambda}(\tilde{T})\partial\tilde{T}/\partial y$ still defines the heat flux density. Fig. 3 shows the temperature mapping and the transformed heat conductivity $\tilde{\lambda}$ if the material parameters from Fig. 2 and $\bar{T}_0 = 273\,\mathrm{K}$ are used. The temperature axes are equally scaled.

2.3. Method of weighted residuals

Consider the Sobolev space $V := H^1(-L/2, L/2)$ and the bilinear form

$$a(v_1, v_2) := \int_{-L/2}^{L/2} v_1 v_2 \mathrm{d}y \;:\; V \times V \to \mathbb{R}. \tag{4}$$

Post-print version of the article: A. Steinboeck, D. Wild, T. Kiefer, and A. Kugi, "A fast simulation method for 1D heat conduction", *Mathematics and Computers in Simulation*, vol. 82, no. 3, pp. 392–403, 2011. DOI: 10.1016/j.matcom.2010.10.016
The content of this post-print version is identical to the published paper but without the publisher's final layout or copy editing.

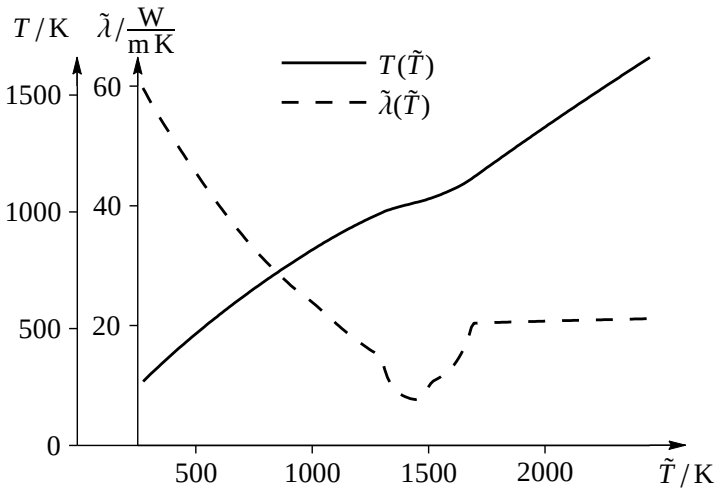

Figure 3: Transformation of temperature and transformed heat conductivity for standard steel (0.1 % carbon).

Using *any* test function $v(y) \in V$ and *any* scalar factors $v^-, v^+ \in \mathbb{R}$, the identity

$$a(v(y), \mathcal{D}(\tilde{T}(y,t))) + v^- \mathcal{B}^-(\tilde{T}(y,t)) + v^+ \mathcal{B}^+(\tilde{T}(y,t)) = 0$$

must hold for any $t > 0$. Here, $\mathcal{D}(\tilde{T}(y,t)) \in L^2(-L/2, L/2)$ and $\|\mathcal{B}^\mp(\tilde{T}(y,t))\| < \infty$ are required, where $L^2(-L/2, L/2)$ is the space of square integrable functions on the interval $(-L/2, L/2)$. The usual way for obtaining the weak formulation is integration by parts (cf. [7, 16]), which yields

$$\begin{aligned} 0 = {} & a\left(v(y), \rho\tilde{c}\frac{\partial \tilde{T}(y,t)}{\partial t}\right) + a\left(\frac{\partial v(y)}{\partial y}, \tilde{\lambda}(\tilde{T}(y,t))\frac{\partial \tilde{T}(y,t)}{\partial y}\right) - v^- q^-(t) - v^+ q^+(t) \\ & - (v^- - v(-L/2))\,\tilde{\lambda}\,\frac{\partial \tilde{T}(y,t)}{\partial y}\bigg|_{y=-L/2} + (v^+ - v(L/2))\,\tilde{\lambda}\,\frac{\partial \tilde{T}(y,t)}{\partial y}\bigg|_{y=L/2} \qquad t > 0. \end{aligned} \tag{5}$$

In this equation, the requirements on the differentiability of $\tilde{T}(y,t)$ with respect to y are less restrictive than in the operator $\mathcal{D}$. Apart from this fact, (3) and (5) are equivalent. Until now, there is no mathematical approximation, implying that the solution of (5) is identical to the solution of the strong formulations (1) and (3).

The basic idea of the MWR is to derive an *approximate* solution of (5) by restricting $\tilde{T}(y,t)$ to some *finite-dimensional* space and by discarding the stipulation that (5) must be satisfied for any $v(y) \in V$ and any $v^-, v^+ \in \mathbb{R}$. A mathematically simple solution may be found if (5) only holds for any $v(y) \in V_h \subseteq V$ and any $v^\mp \in V_h^\mp \subseteq \mathbb{R}$, where V_h is a *finite-dimensional* subspace.

Clearly, the choice $v^\mp = v(\mp L/2)$ causes the second line of (5) to vanish. This reasonable simplification is particularly useful for Neumann boundary conditions [24]. Hence, it is used throughout this paper. Unfortunately, the second term on the right-hand side of (5) contains the generally nonlinear function $\tilde{\lambda}(\tilde{T}(y,t))$. Assuming for the time being that $a(\partial v(y)/\partial y, \partial \tilde{T}(y,t)/\partial y) \neq 0$, the weighted mean value

$$\bar{\lambda} = \bar{\lambda}(v(y), \tilde{T}(y,t)) = \frac{a\left(\frac{\partial v(y)}{\partial y}, \tilde{\lambda}(\tilde{T}(y,t))\frac{\partial \tilde{T}(y,t)}{\partial y}\right)}{a\left(\frac{\partial v(y)}{\partial y}, \frac{\partial \tilde{T}(y,t)}{\partial y}\right)} \tag{6}$$

can be used to rewrite (5) as

$$0 = a\left(v(y), \rho\tilde{c}\frac{\partial \tilde{T}(y,t)}{\partial t}\right) + \bar{\lambda}(v(y), \tilde{T}(y,t))\, a\left(\frac{\partial v(y)}{\partial y}, \frac{\partial \tilde{T}(y,t)}{\partial y}\right) - v(-L/2)\, q^-(t) - v(L/2)\, q^+(t) \qquad t > 0. \tag{7}$$

Note that the parameter $\bar{\lambda}$ does not depend on y. In principle, the introduction of (6) does not entail any approximation error. However, later some accuracy will be sacrificed to simplify time integration. For a computer implementation of the method, special care should be taken to avoid numerical problems if the denominator of (6) is close to zero. For instance, $v(y) = \text{const.}$ or $\tilde{T}(y,t) = \text{const.}$ w.r.t. y should automatically result in $\bar{\lambda} = 0$.

Post-print version of the article: A. Steinboeck, D. Wild, T. Kiefer, and A. Kugi, "A fast simulation method for 1D heat conduction", *Mathematics and Computers in Simulation*, vol. 82, no. 3, pp. 392–403, 2011. DOI: 10.1016/j.matcom.2010.10.016
The content of this post-print version is identical to the published paper but without the publisher's final layout or copy editing.

2.4. Galerkin method

The GM (cf. [8, 16]) is an important subcategory of the MWR. It suggests to approximate the exact solution $\tilde{T}(y,t)$ by $\tilde{T}_h(y,t) \in V_h$, i. e, the finite-dimensional subspace of the approximate solution equals the space of trial functions $V_h := \operatorname{span}\{h_1(y), h_2(y), \ldots, h_H(y)\} \subseteq V$. Thus,

$$\tilde{T}_h(y,t) = \sum_{i=1}^{H} x_i(t) h_i(y). \tag{8}$$

The time dependence of $\tilde{T}$ is reflected by the Galerkin coefficients $x_i(t)$, which can be summarized in the vector $\boldsymbol{x}(t) = [x_1(t), x_2(t), \ldots, x_H(t)]^\mathsf{T}$. The H basis functions $h_i(y) \in V_h$ are used as trial functions, which have to be linearly independent. Moreover, V_h can be chosen such that some homogeneous boundary conditions are automatically satisfied by $\tilde{T}_h(y,t)$. However, for the considered problem, the boundary conditions are generally inhomogeneous.

Evaluation of (7) for the H trial functions $h_i(y)$ ($v(y)$ is replaced by $h_i(y)$) yields an initial-value problem in form of an explicit ODE for the unknown Galerkin coefficients $\boldsymbol{x}(t)$. Therefore, $\boldsymbol{x}(t)$ are the states of a dynamical system of order H. It is referred to as lumped-parameter system. In line with the MWR, it seems reasonable to obtain the initial values $\boldsymbol{x}(0) = \boldsymbol{x}_0$ by minimizing the deviation between $\tilde{T}_h(y,0)$ and the given initial temperature profile $\tilde{T}(T_0(y))$ weighted by the trial functions $h_i(y)$. Therefore, $a(h_i(y), \tilde{T}_h(y,0) - \tilde{T}(T_0(y))) = 0 \;\forall\, i \in \{1, 2, \ldots, H\}$. Insertion of (8) and utilization of the linearity of $a(v_1, v_2)$ (cf. (4)) yield the linear equation

$$\begin{bmatrix} a(h_1(y), h_1(y)) & \cdots & a(h_1(y), h_H(y)) \\ \vdots & \ddots & \vdots \\ a(h_H(y), h_1(y)) & \cdots & a(h_H(y), h_H(y)) \end{bmatrix} \boldsymbol{x}_0 = \begin{bmatrix} a(h_1(y), \tilde{T}(T_0(y))) \\ \vdots \\ a(h_H(y), \tilde{T}(T_0(y))) \end{bmatrix}. \tag{9}$$

Since linear independence of the basis functions $h_i(y)$ was assumed, (9) can be readily solved for the initial state $\boldsymbol{x}_0$.

In the sequel, the proposed approach is explained with a three-dimensional *orthogonal* basis

$$h_1(y) = 1, \qquad h_2(y) = \frac{2y}{L}, \qquad h_3(y) = \left(\frac{2y}{L}\right)^2 - \frac{1}{3}, \tag{10}$$

i. e. $H = 3$ and $\tilde{T}_h(y,t)$ is a quadratic polynomial in y. The rationale for this choice is that—given the right initial condition $\tilde{T}(T_0(y))$—it would allow an *exact* solution of (3) if $\tilde{\lambda}$, $q^-(t)$, and $q^+(t)$ were constant. For an arbitrary initial condition $\tilde{T}(T_0(y))$, the error would converge to zero. Even for non-constant material parameters or heat fluxes, the chosen trial functions prove useful. In Section 3, it will be demonstrated that for the intended application, (10) facilitates an acceptable balance between computational effort and achieved accuracy. Adding additional polynomial trial functions, i. e. $H > 3$, is possible in an analogous way. Corresponding results will be shown in Section 3.

Substitution of (10) and (8) into (7) for $v = h_1$, $v = h_2$, and $v = h_3$ yields

$$\dot{\boldsymbol{x}}(t) = \boldsymbol{A}(\boldsymbol{x}(t))\boldsymbol{x}(t) + \boldsymbol{B}\boldsymbol{q}(t) \qquad t > 0 \tag{11a}$$

with the initial value $\boldsymbol{x}(0) = \boldsymbol{x}_0$, the heat flux inputs $\boldsymbol{q}(t) = [q^-(t), q^+(t)]^\mathsf{T}$, and the matrices

$$\boldsymbol{A} = -\frac{12}{\rho \tilde{c} L^2} \operatorname{diag}\left\{0 \quad \bar{\lambda}(h_2, \tilde{T}_h) \quad 5\bar{\lambda}(h_3, \tilde{T}_h)\right\} \tag{11b}$$

$$\boldsymbol{B} = \frac{1}{\rho \tilde{c} L} \operatorname{diag}\left\{1 \quad 3 \quad {}^{15}\!/_{2}\right\} \begin{bmatrix} 1 & 1 \\ -1 & 1 \\ 1 & 1 \end{bmatrix}. \tag{11c}$$

Note that the ODE (11) is generally *nonlinear* because $\boldsymbol{A}$ contains the parameters $\bar{\lambda}(h_2, \tilde{T}_h)$ and $\bar{\lambda}(h_3, \tilde{T}_h)$ with $\tilde{T}_h$ from (8). The computation of these parameters requires two evaluations of (6) at each time integration point. The favorable property that $\boldsymbol{A}$ exhibits a diagonal structure is lost if $H > 3$, however, the method proceeds in the same way.

A substitution of the heat input $\boldsymbol{q}(t)$ in (11a) by the expression for the radiative heat exchange would introduce a significant nonlinearity to the system because $q^-(t)$ and $q^+(t)$ depend on the surface temperatures $T(\tilde{T}_h(-L/2, t))$ and $T(\tilde{T}_h(L/2, t))$, respectively. Therefore, the consideration of radiative heat exchange is postponed until a discrete-time system is obtained.

Post-print version of the article: A. Steinboeck, D. Wild, T. Kiefer, and A. Kugi, "A fast simulation method for 1D heat conduction", *Mathematics and Computers in Simulation*, vol. 82, no. 3, pp. 392–403, 2011. DOI: 10.1016/j.matcom.2010.10.016
The content of this post-print version is identical to the published paper but without the publisher's final layout or copy editing.

2.5. FOH-type time integration method

Any standard numerical ODE solver algorithm for explicit initial-value problems should suffice to integrate (11). However, the benefit of manual discretization of the system is that usually laborious iterative solver algorithms can be replaced by algebraic difference equations, which allow rapid evaluation. Consider a discretized time domain with sampling instants $t_k \; \forall\, k \in \mathbb{N}$, which are generally *not* equidistant, and let $T_k = t_{k+1} - t_k$ be the corresponding sampling period.

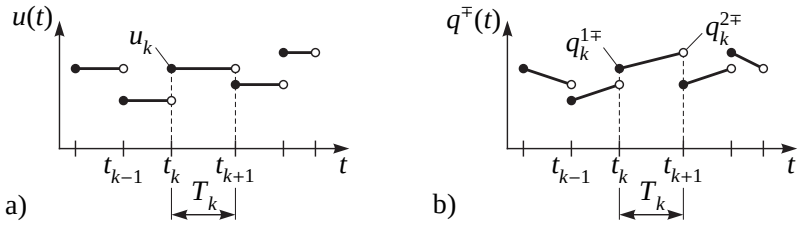

Figure 4: Shape of input signal, a) ZOH method, b) FOH-type method.

In order to obtain a discrete-time representation [9, 14] of a state space system like (11), the Zero-Order-Hold (ZOH) method [9, 15] is frequently applied. ZOH means that any input is forced to a function space which has the step functions $\sigma(t-t_k) \; \forall\, k \in \mathbb{N}$ as a basis, as exemplified in Fig. 4.a for some scalar input $u(t)$. Inspired by the fact that the First-Order-Hold (FOH) method [9, 15] furnishes more accurate results than the ZOH method, a time integration method capable of *piecewise linear* input signals is outlined in the following. Moreover, the considered function space allows for *discontinuous* input signals, which may occur in process control applications. Sampling points t_k must be set at least at discontinuities of the input signals or their slope. Then, the input $\boldsymbol{q}(t)$ of (11a) can be defined as

$$\boldsymbol{q}(t) = \boldsymbol{q}_k^1 \frac{t_{k+1} - t}{T_k} + \boldsymbol{q}_k^2 \frac{t - t_k}{T_k} \qquad \text{for} \qquad t_k \le t < t_{k+1} \tag{12}$$

with $\boldsymbol{q}_k^1 = [q_k^{1-}, q_k^{1+}]^\mathsf{T}$ and $\boldsymbol{q}_k^2 = [q_k^{2-}, q_k^{2+}]^\mathsf{T}$. The meaning of these vectors is illustrated in Fig. 4.b. However, the components $q^-(t)$ and $q^+(t)$ are generally not equal. The vectors may be obtained from

$$\boldsymbol{q}_k^1 = \boldsymbol{q}(t_k), \qquad \boldsymbol{q}_k^2 = \lim_{\tau \to 0^-} \boldsymbol{q}(t_{k+1} + \tau).$$

The series $(\boldsymbol{q}_k^1)$ and $(\boldsymbol{q}_k^2)$ are the inputs to the discretized system. In order to facilitate a simple analytical solution of the ODE (11), it is assumed that the parameters $\bar{\lambda}(h_2, \tilde{T}_h)$ and $\bar{\lambda}(h_3, \tilde{T}_h)$ take the *constant* values $\bar{\lambda}(h_2, \tilde{T}_h(y, t_k))$ and $\bar{\lambda}(h_3, \tilde{T}_h(y, t_k))$ within each time interval $[t_k, t_{k+1})$. Implementing this *approximation*, the integration of (11) with the input (12) readily yields the discrete-time system

$$\boldsymbol{x}_{k+1} = \boldsymbol{A}_k(\boldsymbol{x}_k)\boldsymbol{x}_k + \boldsymbol{B}_k^1(\boldsymbol{x}_k)\boldsymbol{q}_k^1 + \boldsymbol{B}_k^2(\boldsymbol{x}_k)\boldsymbol{q}_k^2 \tag{13a}$$

with

$$\boldsymbol{A}_k = \operatorname{diag}\left\{1 \quad \exp\left(\frac{-12\bar{\lambda}(h_2,\tilde{T}_h(y,t_k))T_k}{\rho\check{c}L^2}\right) \quad \exp\left(\frac{-60\bar{\lambda}(h_3,\tilde{T}_h(y,t_k))T_k}{\rho\check{c}L^2}\right)\right\} \tag{13b}$$

$$\boldsymbol{B}_k^1 = \operatorname{diag}\left\{\begin{array}{l} \frac{T_k}{2\rho\check{c}L} \\ \frac{L}{4\bar{\lambda}(h_2,\tilde{T}_h(y,t_k))}\left(-1 + \left(1 + \frac{\rho\check{c}L^2}{12\bar{\lambda}(h_2,\tilde{T}_h(y,t_k))T_k}\right)\left(1 - \exp\left(\frac{-12\bar{\lambda}(h_2,\tilde{T}_h(y,t_k))T_k}{\rho\check{c}L^2}\right)\right)\right) \\ \frac{L}{8\bar{\lambda}(h_3,\tilde{T}_h(y,t_k))}\left(-1 + \left(1 + \frac{\rho\check{c}L^2}{60\bar{\lambda}(h_3,\tilde{T}_h(y,t_k))T_k}\right)\left(1 - \exp\left(\frac{-60\bar{\lambda}(h_3,\tilde{T}_h(y,t_k))T_k}{\rho\check{c}L^2}\right)\right)\right) \end{array}\right\} \begin{bmatrix} 1 & 1 \\ -1 & 1 \\ 1 & 1 \end{bmatrix} \tag{13c}$$

$$\boldsymbol{B}_k^2 = \operatorname{diag}\left\{\begin{array}{l} \frac{T_k}{2\rho\check{c}L} \\ \frac{L}{4\bar{\lambda}(h_2,\tilde{T}_h(y,t_k))}\left(1 - \frac{\rho\check{c}L^2}{12\bar{\lambda}(h_2,\tilde{T}_h(y,t_k))T_k}\left(1 - \exp\left(\frac{-12\bar{\lambda}(h_2,\tilde{T}_h(y,t_k))T_k}{\rho\check{c}L^2}\right)\right)\right) \\ \frac{L}{8\bar{\lambda}(h_3,\tilde{T}_h(y,t_k))}\left(1 - \frac{\rho\check{c}L^2}{60\bar{\lambda}(h_3,\tilde{T}_h(y,t_k))T_k}\left(1 - \exp\left(\frac{-60\bar{\lambda}(h_3,\tilde{T}_h(y,t_k))T_k}{\rho\check{c}L^2}\right)\right)\right) \end{array}\right\} \begin{bmatrix} 1 & 1 \\ -1 & 1 \\ 1 & 1 \end{bmatrix}. \tag{13d}$$

Post-print version of the article: A. Steinboeck, D. Wild, T. Kiefer, and A. Kugi, “A fast simulation method for 1D heat conduction”, *Mathematics and Computers in Simulation*, vol. 82, no. 3, pp. 392–403, 2011. DOI: 10.1016/j.matcom.2010.10.016
The content of this post-print version is identical to the published paper but without the publisher’s final layout or copy editing.

Strictly speaking, (13) is non-causal, since $\boldsymbol{q}_k^2$ occurs at the same time as $\boldsymbol{x}_{k+1}$. Moreover, it is generally *nonlinear* because the system matrices depend on $\tilde{T}_h(y, t_k)$. The system is *time-variant* if the sampling period T_k is not constant. The favorable diagonal structure of $\boldsymbol{A}_k$ is lost if $H > 3$.

To show that the FOH integration method [15] is a special case of the approach proposed above, consider a linear time-invariant system with the transfer function $G(s)$, equidistant sampling time, i. e. $T_k = \text{const.}$, and a continuous scalar input. Let, s be the Laplace variable and z the complex variable of the Z-transform. Then, the familiar transformation equation [9]

$$G_z(z) = \frac{(z-1)^2}{z} \mathrm{Z}\left\{ G(s) \frac{1}{s^2 T_k} \right\}$$

for the Z-transfer function $G_z(z)$ is obtained. Here, $\mathrm{Z}\{\cdot\}$ represents the transition from the (continuous) Laplace domain to the (discrete) Z-domain by means of inverse Laplace transformation, sampling of the obtained time signal, and Z-transform of the resulting series.

The benefit of the proposed integration scheme compared to the classical ZOH or FOH method is that complicated input signals with non-equidistant discontinuities can be approximated more accurately. Therefore, the analysis is continued using the discrete-time system (13).

2.6. Radiative heat exchange

The boundary conditions are defined by two decoupled radiation problems in the volumes below and above the domain $[-L/2, L/2]$. Consider in Fig. 1 the top/bottom wall surface as well as the surface $y = \mp L/2$, which are separated by a *non-participating* medium, meaning that the medium does *not* emit thermal radiation and any rays passing the medium are neither *scattered* nor *absorbed* or *attenuated*. This assumption is acceptable for pure air and if the distances between the considered surfaces do not exceed a few meters. However, for other media or for hot atmospheres, like they may appear in the steel industry, the assumption is likely to be unjustified (cf. [11, 12, 13]). Frequently, a reliable measurement of the gas temperature is not available whereas wall surface temperatures can be measured with higher reliability. Consequently, the wall surface temperatures serve as *control inputs*, which are commonly governed by cascade control loops (cf. [6, 18, 23]). Therefore, the gaseous atmosphere between the radiating surfaces is disregarded in this analysis. Model parameters, like the emissivity, are adjusted to compensate at least partially for the error introduced by the restrictive assumption of a non-participating medium.

Let the two involved surfaces be diffuse gray bodies with emissivities $\varepsilon_w^{\mp}$ and $\varepsilon^{\mp}$, respectively and assume that the temperature distribution on the surfaces is homogeneous. Then, the net heat flux density between the wall and the surface $y = \mp L/2$ is obtained as

$$q^{\mp}(t) = \frac{\sigma}{\dfrac{\varepsilon^{\mp} + \varepsilon_w^{\mp}}{\varepsilon^{\mp}\varepsilon_w^{\mp}} - 1} \left((T_w^{\mp})^4(t) - T^4\left(\mp L/2, t\right) \right), \tag{14}$$

where the Stefan-Boltzmann law and Kirchhoff's law of thermal radiation have been used [11, 12, 13]. Here, $\sigma = (5.670\,400 \pm 0.000\,040) \times 10^{-8} \frac{\mathrm{W}}{\mathrm{m^2 K^4}}$ is the Stefan-Boltzmann constant. The surface temperature $T(\mp L/2, t)$ in (14) is replaced by its Galerkin approximation $T(\tilde{T}_h(\mp L/2, t)) = T([1,\ \mp 1,\ 2/3]\boldsymbol{x}(t))$. The evaluation of (14) at the sampling points t_k and t_{k+1} allows to derive the input values $q_k^{1\mp}$ and $q_k^{2\mp}$ of the discrete-time system (13) as

$$q_k^{1\mp} = \frac{\sigma}{\dfrac{\varepsilon^{\mp} + \varepsilon_w^{\mp}}{\varepsilon^{\mp}\varepsilon_w^{\mp}} - 1} \left(\lim_{\tau \to 0^+} \left((T_w^{\mp})^4(t_k + \tau) \right) - T^4\left(\begin{bmatrix} 1 & \mp 1 & 2/3 \end{bmatrix} \boldsymbol{x}_k \right) \right) \tag{15a}$$

$$q_k^{2\mp} = \frac{\sigma}{\dfrac{\varepsilon^{\mp} + \varepsilon_w^{\mp}}{\varepsilon^{\mp}\varepsilon_w^{\mp}} - 1} \left(\lim_{\tau \to 0^-} \left((T_w^{\mp})^4(t_{k+1} + \tau) \right) - T^4\left(\begin{bmatrix} 1 & \mp 1 & 2/3 \end{bmatrix} \boldsymbol{x}_{k+1} \right) \right). \tag{15b}$$

The one-sided limits in (15) are necessary to allow for discontinuous input signals $T_w^{\mp}(t)$. At first sight, this may seem implausible since surface temperatures cannot jump. However, the approach is suitable for batch processes or discontinuous process steps, where the solid is quickly shifted into a new environment. Therefore, $T_w^{\mp}(t)$ may be regarded as an ambient temperature referring to the current environment of the solid.

Post-print version of the article: A. Steinboeck, D. Wild, T. Kiefer, and A. Kugi, "A fast simulation method for 1D heat conduction", *Mathematics and Computers in Simulation*, vol. 82, no. 3, pp. 392–403, 2011. DOI: 10.1016/j.matcom.2010.10.016
The content of this post-print version is identical to the published paper but without the publisher's final layout or copy editing.

2.7. Implicit system

Insertion of (15b) into (13a) yields an *implicit* algebraic equation

$$\boldsymbol{x}_{k+1} = \boldsymbol{f}(\boldsymbol{x}_{k+1}) \tag{16}$$

for the unknown state $\boldsymbol{x}_{k+1}$. Obviously, $\boldsymbol{f}(\boldsymbol{x}_{k+1})$ depends on $\boldsymbol{A}_k$, $\boldsymbol{B}_k^1$, $\boldsymbol{B}_k^2$, $\boldsymbol{x}_k$, $\boldsymbol{q}_k^1$, σ, $\varepsilon^{\mp}$, $\varepsilon_w^{\mp}$, the transformation $T(\tilde{T})$, and the left-sided limit of $T_w^{\mp}(t)$ at $t = t_{k+1}$.

For usual parameter values and reasonable choices of the sampling period T_k, $\boldsymbol{f} : \mathbb{R}^H \to \mathbb{R}^H$ is a *local* contraction [3], meaning that it is locally Lipschitz continuous with a Lipschitz constant $K \in (0, 1)$. Since $K \ll 1$ is observed in most cases, the fixed-point iteration method [3] suggests itself as an iterative routine for solving the implicit equation. However, its convergence behavior depends on the chosen sampling period and is only *linear*. Thus, for expedited computation, it is recommended to utilize the Newton-Raphson method, which exhibits *quadratic* convergence. If a chosen starting point inhibits the convergence of the Newton-Raphson method, it may be worth using relaxed Newton-Raphson methods (variable step length), returning to the fixed-point iteration method, or reducing the chosen sampling period. Generally, the proposed mathematical model is favorable insofar as for both iterative solution methods the value of $\boldsymbol{x}_k$ proved to be a good starting point to search for $\boldsymbol{x}_{k+1}$. Convergence problems have not been observed, even for coarse discretization of the time domain, as will be demonstrated in the following section.

3. Example problem

The proposed method is used to compute the temperature field in a steel slab which undergoes heat treatment in some radiative environment as outlined in Fig. 1. The influence of the chosen sampling period T_k is studied, and numerical results are compared to values obtained by the FDM. In conventional reheating furnaces, it takes approximately 6 h until steel slabs acquire their desired processing temperatures above 1350 K. However, the reheating time depends strongly on the geometric dimensions and material properties of the slab.

The slab to be analyzed in this example has a homogeneous initial temperature $T_0(y) = 300\,\mathrm{K}$, a thickness of $L = 0.5\,\mathrm{m}$, and surface emissivities of $\varepsilon^- = 0.65$ and $\varepsilon^+ = 0.75$ at the surfaces $y = -L/2$ and $y = L/2$, respectively. The smaller value at the bottom surface may be considered as a compensation for the shade caused by some support (not shown in Fig. 1) which holds the slab in place. Values of the temperature-dependent material parameters $c(T)$ and $\lambda(T)$ are defined in Fig. 2. The enclosing surfaces have the emissivity $\varepsilon_w^- = \varepsilon_w^+ = 0.7$. Their temperatures

$$T_w^-(t) = \begin{cases} 1600\,\mathrm{K} & \text{if } t < 12\,\mathrm{h} \\ 300\,\mathrm{K} & \text{else} \end{cases}, \qquad T_w^+(t) = \begin{cases} 1600\,\mathrm{K} & \text{if } t < 6\,\mathrm{h} \\ 300\,\mathrm{K} & \text{else} \end{cases},$$

serve as inputs. In real applications, significant differences between the environmental temperatures below and above the slab, like in the interval from 6 h to 12 h, may occur in hearth type furnaces. However, here, the input ambient temperatures are chosen to represent a challenging example with respect to the numerical solution of the problem.

An exact analytical solution of the problem has not been found. Therefore, the results of a standard FDM algorithm implemented in the MATLAB® command `pdepe` [19] are used as a *reference solution*. The number of equidistant spatial grid points is chosen as $N = 100$, whereas time stepping is adaptive. For time integration, the `pdepe` command uses a variable order multistep solver, which realizes Gear's method [17]. In the following, the deviation between an approximate temperature result T_h and a reference result T will be denoted as $\Delta T = T_h - T$.

For comparison, the ODE obtained from the FDM is also integrated with the implicit Crank-Nicolson method [5] executed at fixed time steps. Like for the proposed FOH-type integration scheme (cf. Section 2.7), the Crank-Nicolson approach requires to solve an implicit algebraic equation at each sampling instant. It is emphasized that explicit integration methods, which are computationally easier to handle, would significantly limit the sampling time because of possible numerical instability. It is an advantage of the FDM that it can be applied directly to the heat conduction equation (1), i. e. the transformation proposed in Section 2.2 is not required. To make the results comparable to the proposed GM with H trial functions, the FDM is computed with $N = H$ equidistant grid points.

Post-print version of the article: A. Steinboeck, D. Wild, T. Kiefer, and A. Kugi, "A fast simulation method for 1D heat conduction", *Mathematics and Computers in Simulation*, vol. 82, no. 3, pp. 392–403, 2011. DOI: 10.1016/j.matcom.2010.10.016
The content of this post-print version is identical to the published paper but without the publisher's final layout or copy editing.

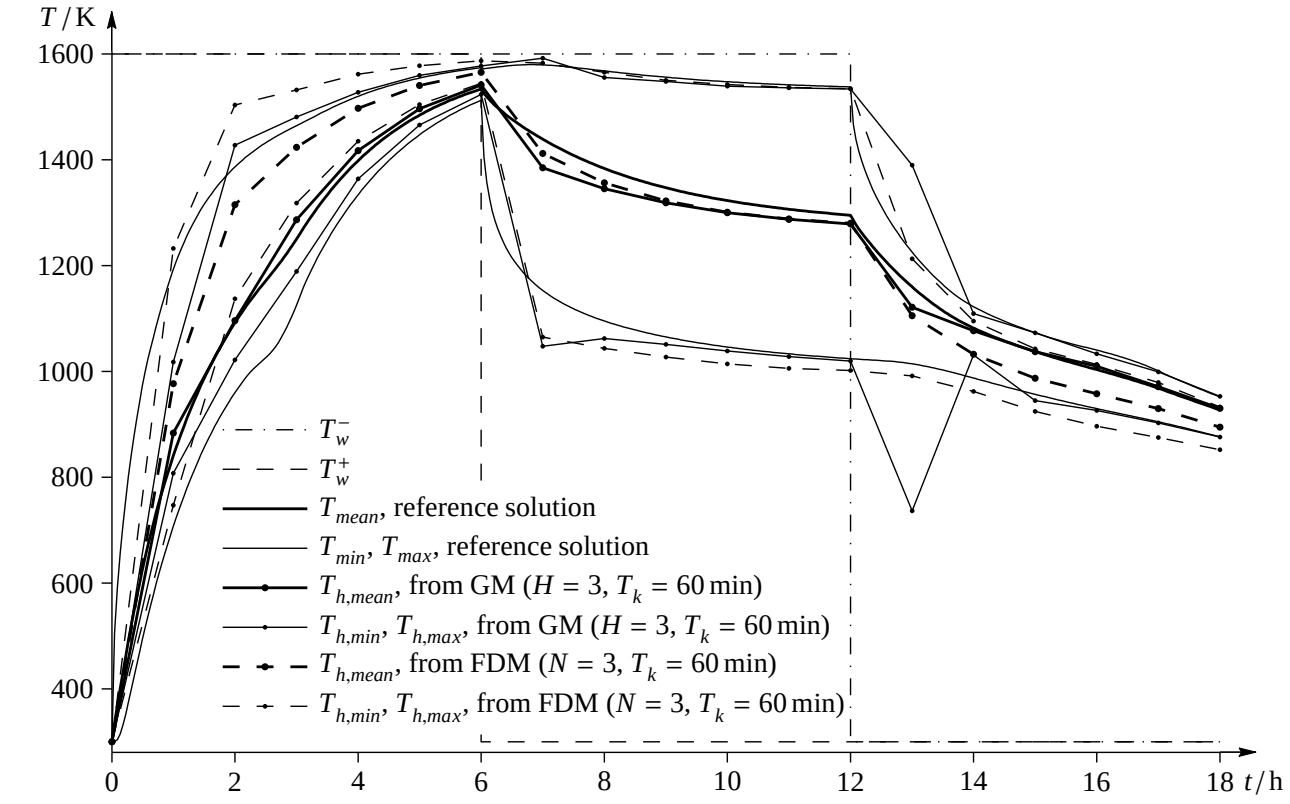

Figure 5: Input ambient temperatures and minimum, mean, and maximum temperature of the solid.

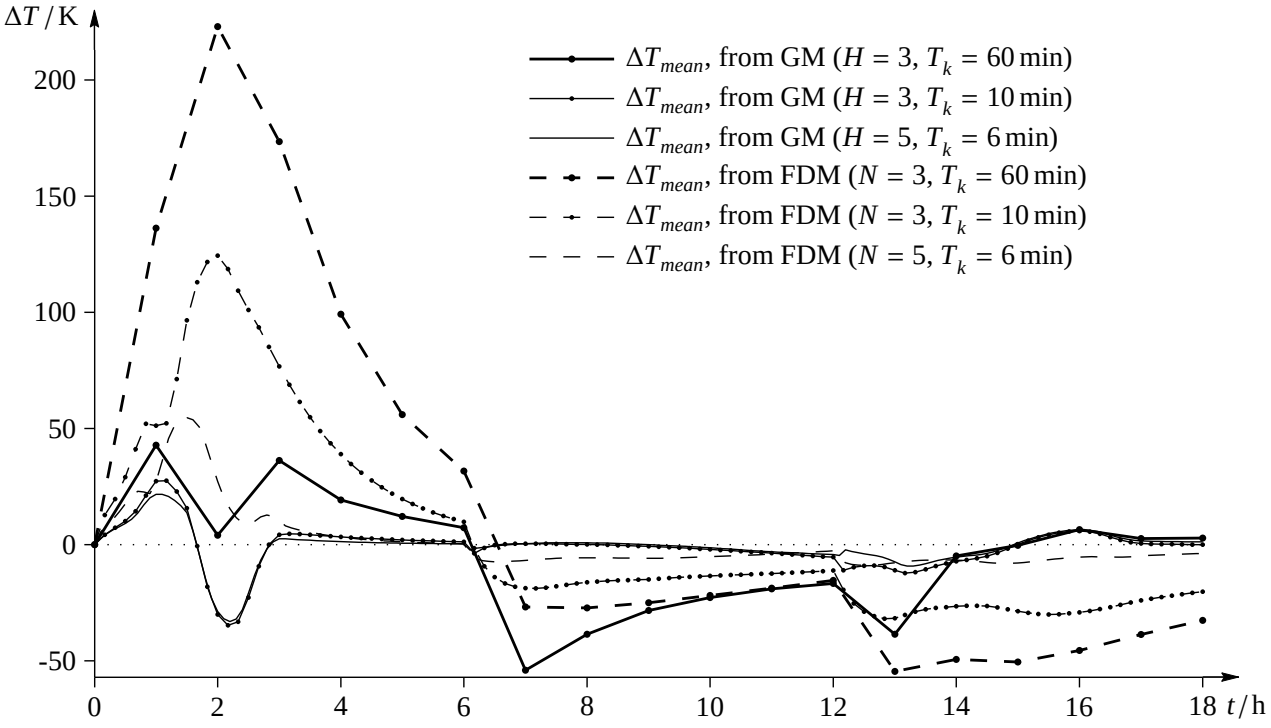

Figure 6: Deviation between the approximate mean temperature and the reference solution.

Post-print version of the article: A. Steinboeck, D. Wild, T. Kiefer, and A. Kugi, "A fast simulation method for 1D heat conduction", *Mathematics and Computers in Simulation*, vol. 82, no. 3, pp. 392–403, 2011. DOI: 10.1016/j.matcom.2010.10.016
The content of this post-print version is identical to the published paper but without the publisher's final layout or copy editing.

Together with the inputs and the reference solution, numerical results computed by means of both the proposed GM with the FOH-type integration method and the FDM with the Crank-Nicolson integration scheme are shown in Fig. 5. It contains the minimum, the maximum, and the mean value of the temperature profile for each sampling period. To keep the figure uncluttered, only results for a fixed sampling time $T_k = 60\,\mathrm{min}$ are shown. It is possible to further increase the sampling period, however, the achieved accuracy obviously deteriorates.

Two major sources of inaccuracies are the discretization of the spatial domain and the time domain. Refining the resolution of only one of these dimensions is less effective than refining the resolution of both dimensions at the same time. For the GM this would mean to increase H, the number of trial functions, which entails an increase in terms of the computational load. Therefore, in this analysis, H never exceeds 5.

The deviations ΔT_{mean} between the mean temperatures of the approximate results and the mean temperature of the reference solution are shown in Fig. 6 for various H, N, and T_k. The FDM with small N underestimates the thermal inertia of the system, whereas with the GM this is only the case for large sampling periods T_k. Evidently, the improvement from $H = 3$ to $H = 5$ is only moderate.

The GM produces the largest deviations right after discontinuous changes of the inputs. However, the practical relevance of these transient errors is rather marginal. Moreover, the errors can be easily reduced if the sampling periods T_k are decreased in the vicinity of discontinuous changes of the inputs.

In this analysis, $\bar{\lambda}(h_i, \tilde{T}_h(y,t))$ is considered to be constant during the interval $[\,t_k, t_{k+1})$ and it depends only on $\boldsymbol{x}_k$ and $i \in \{1, 2, \ldots, H\}$. Therefore, the accuracy could be further improved if both $\boldsymbol{x}_k$ and $\boldsymbol{x}_{k+1}$ were utilized in the computation of $\bar{\lambda}$ for the interval $[\,t_k, t_{k+1})$. For simplicity, this idea was not followed in this work.

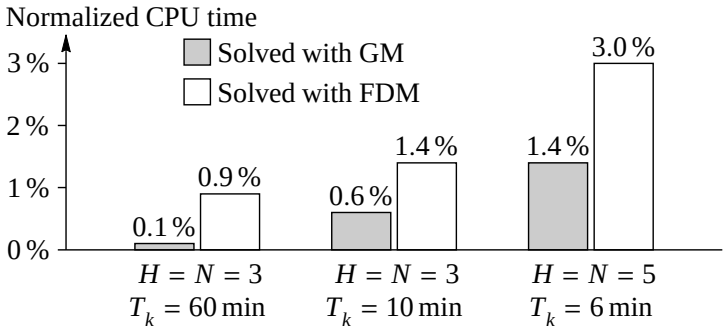

Figure 7: Required computation time normalized with respect to the computation time of the reference solution.

The influence of H, N, and T_k on the computation time is summarized in Fig. 7. Generally, the results of the GM with the FOH-type integration scheme are in terms of both *accuracy* and *computational load* superior to the results of the FDM with a fixed-step integration scheme.

The example problem demonstrates the virtues of the proposed method. The obtained system is low-dimensional—it has H states. The accuracy achieved with $H = 3$ is very acceptable for many applications in the steel industry, even if the sampling times T_k are in excess of 1 h. Variations of the sampling period do not limit the applicability of the method since each time interval is integrated individually.

4. Discussion

A method for computing the transient temperature field in a solid with nonlinear material parameters subjected to radiative heat inputs was proposed. Important *principles* adopted in the course of the analysis are:

- the postponement of nonlinear radiation boundary conditions (14) by employing Neumann boundary conditions (1c) until the discretized system (13) is obtained,
- a nonlinear, bijective, time-invariant transformation (2) of the temperature to simplify the consideration of nonlinear material parameters c and λ,
- the GM with $H = 3$ trial functions (10) to derive a lumped-parameter system (11),
- and an FOH-type time integration method to discretize the time domain (cf. (13)).

Post-print version of the article: A. Steinboeck, D. Wild, T. Kiefer, and A. Kugi, "A fast simulation method for 1D heat conduction", *Mathematics and Computers in Simulation*, vol. 82, no. 3, pp. 392–403, 2011. DOI: 10.1016/j.matcom.2010.10.016
The content of this post-print version is identical to the published paper but without the publisher's final layout or copy editing.

Finally, the implicit algebraic equation (16) is obtained, which can be solved without difficulty. The most salient *modeling assumptions* materialized in this work can be summarized as follows:

- The geometries of the solid and the ambient surfaces are considered infinitely large along two spatial dimensions. The temperature field is assumed to be constant along these directions. The approximation seems justified if the length and the width of the solid significantly exceed its thickness L or if many solids are densely arranged side by side.
- For the formulation of radiation boundary conditions, it is assumed that the surfaces are separated by a non-participating gaseous medium.
- The surfaces themselves are considered as diffuse gray bodies with homogeneous temperatures and constant emissivities $\varepsilon_w^{\mp}$ and $\varepsilon^{\mp}$.

However, modeling assumptions are not the only compromise made in this analysis—there are also some significant *mathematical approximations*:

- The MWR suggests to approximate the temperature field $\tilde{T}(y,t)$ by $\tilde{T}_h(y,t)$ taken from some finite-dimensional space. In this paper, the GM was utilized, where $\tilde{T}_h(y,t)$ and the trial functions $v(y)$ are confined to the same space V_h. A reasonable choice for the trial functions h_i ($i \in \{1,2,\ldots,H\}$) is vital for minimizing the entailed approximation error.
- It is assumed that $\overline{\lambda}(h_i,\tilde{T}_h)\ \forall\, i \in \{1,2,\ldots,H\}$ in (11b) takes the constant value $\overline{\lambda}(h_i,\tilde{T}_h(y,t_k))$ during each time interval $[t_k,t_{k+1})$.
- The input $\boldsymbol{q}(t)$ is constrained to a piecewise linear signal (12), which may jump at t_k. Therefore, sampling points t_k should be set at least at discontinuities of $\boldsymbol{q}(t)$.
- The radiation boundary conditions (14) are only satisfied at the sampling points t_k, since they have been introduced after discretization of the time domain. For their computation, the surface temperature $T(\mp L/2,t_k)$ is replaced by its Galerkin approximation.
- The implicit difference equation (16) is only numerically solved.

Despite these limitations, the proposed method proved to be adequate for many purposes, especially the intended application in the steel industry.

Compared to the FDM, the GM yields a mathematical structure that is beneficial for control tasks. The *mean* of the transformed temperature $\tilde{T}$ and, for $H = 2$ or $H = 3$, the *symmetry* of the current temperature profile are reflected by the single state variables $x_1(t)$ and $x_2(t)$ or $x_{1,k}$ and $x_{2,k}$ for the continuous-time or discrete-time system, respectively. Neglecting the temperature dependence of $\lambda(h_i,\tilde{T}_h(y,t_k))$ in (11b), which, anyhow, is weak, $x_1(t)$ and $x_2(t)$ are independent states of (11a), since $\boldsymbol{A}$ exhibits a diagonal structure. Moreover, the structure of $\boldsymbol{B}$ suggests the regular input transformation

$$\boldsymbol{q}(t) = \begin{bmatrix} q^-(t) \\ q^+(t) \end{bmatrix} = \frac{1}{2}\begin{bmatrix} 1 & -1 \\ 1 & 1 \end{bmatrix}\begin{bmatrix} q_1(t) \\ q_2(t) \end{bmatrix}$$

to obtain two *decoupled* systems, where $q_1(t)$ controls only $x_1(t)$ and $q_2(t)$ only $x_2(t)$. If the (stable) state $x_3(t)$ is ignored as an output, the two systems are of the single-input single-output type. Compared to the FDM, this approach significantly simplifies the design of a temperature controller which uses the ambient temperatures as inputs, because the original multi-input multi-output system (11) simplifies to two independent single-input single-output systems. The same input transformation can be applied without effort to the discrete-time system (13).

Some more advantages of the proposed method are acceptable accuracy with only three Galerkin trial functions (10), even for large sampling periods, robustness against variations of the sampling time, reliable convergence behavior, small model dimensions, and low computational costs. The latter properties may be of particular interest if the model should be used in real-time applications. Therefore, the proposed method can be suitable for implementations in trajectory planning, optimization, or control tasks, where constraints on the computing time are often tight.

Acknowledgments

The authors from Vienna University of Technology thankfully acknowledge the sustained support provided by AG der Dillinger Hüttenwerke.

Post-print version of the article: A. Steinboeck, D. Wild, T. Kiefer, and A. Kugi, "A fast simulation method for 1D heat conduction", *Mathematics and Computers in Simulation*, vol. 82, no. 3, pp. 392–403, 2011. DOI: 10.1016/j.matcom.2010.10.016
The content of this post-print version is identical to the published paper but without the publisher's final layout or copy editing.

References

[1] H. D. Baehr, K. Stephan, Heat and Mass Transfer, 2nd ed., Springer-Verlag, Berlin Heidelberg, 2006.

[2] L. Balbis, J. Balderud, M. J. Grimble, Nonlinear predictive control of steel slab reheating furnace, Proceedings of the American Control Conference, Seattle, Washington, USA (2008) 1679–1684.

[3] V. Berinde, Iterative Approximation of Fixed Points, vol. 1912 of Lecture Notes in Mathematics, Springer, Berlin, 2007.

[4] BISRA, Physical constants of some commercial steels at elevated temperatures, Tech. rep., British Iron & Steel Research Association, London (1953).

[5] J. Crank, P. Nicholson, A practical method for numerical evaluation of solutions of partial differential equations of the heat conduction type, Proc. Cambridge Philos. Soc. 43 (1947) 50–67.

[6] G. v. Ditzhuijzen, D. Staalman, A. Koorn, Identification and model predictive control of a slab reheating furnace, Proceedings of the 2002 IEEE International Conference on Control Applications, Glasgow, UK (2002) 361–366.

[7] L. C. Evans, Partial Differential Equations, vol. 19 of Graduate Studies in Mathematics, American Mathematical Society, Providence, Rhode Island, 2002.

[8] C. Fletcher, Computational Galerkin Methods, Springer, New York, 1984.

[9] G. F. Franklin, J. D. Powell, M. Workman, Digital Control of Dynamic Systems, 3rd ed., Prentice Hall, Upper Saddle River, 1997.

[10] K. Harste, Untersuchung zur Schrumpfung und zur Entstehung von mechanischen Spannungen während der Erstarrung und nachfolgender Abkühlung zylindrischer Blöcke aus Fe-C-Legierungen, Ph.D. thesis, Technische Universität Clausthal (1989).

[11] H. C. Hottel, A. F. Sarofim, Radiative Transfer, McGraw-Hill, New York, 1967.

[12] J. H. Lienhard IV, J. H. Lienhard V, A Heat Transfer Textbook, 3rd ed., Phlogiston Press, Cambridge, Massachusetts, 2002.

[13] M. F. Modest, Radiative Heat Transfer, 2nd ed., Academic Press, New York, 2003.

[14] K. Ogata, Discrete-Time Control Systems, 2nd ed., Prentice Hall, Upper Saddle River, 1995.

[15] C. Philipps, H. Nagle, Digital Control System Analysis and Design, 3rd ed., Prentice Hall, Englewood Cliffs, 1995.

[16] B. D. Reddy, Introductory Functional Analysis, Texts in Applied Mathematics, Springer, New York, 1997.

[17] L. F. Shampine, M. W. Reichelt, J. A. Kierzenka, Solving index-1 DAEs in MATLAB and Simulink, SIAM Review 41 (1999) 538–552.

[18] H. Sibarani, Y. Samyudia, Robust nonlinear slab temperature control design for an industrial reheating furnace, Computer Aided Chemical Engineering 18 (2004) 811–816.

[19] R. D. Skeel, M. Berzins, A method for the spatial discretization of parabolic equations in one space variable, SIAM Journal on Scientific and Statistical Computing 11 (1990) 1–32.

[20] A. Steinboeck, D. Wild, T. Kiefer, A. Kugi, A flexible time integration method for the 1D heat conduction problem, Proceedings of the 6th Vienna Conference on Mathematical Modelling, Vienna, Austria, ARGESIM Report no. 35 (2009) 1204–1214.

[21] D. Wild, T. Meurer, A. Kugi, Modelling and experimental model validation for a pusher-type reheating furnace, Mathematical and Computer Modelling of Dynamical Systems 15 (3) (2009) 209–232.

[22] N. Yoshitani, T. Ueyama, M. Usui, Optimal slab heating control with temperature trajectory optimization, Proceedings of the 20th International Conference on Industrial Electronics, Control and Instrumentation, IECON'94 3 (1994) 1567–1572.

[23] B. Zhang, Z. Chen, L. Xu, J. Wang, J. Zhang, H. Shao, The modeling and control of a reheating furnace, Proceedings of the American Control Conference, Anchorage, Alaska, USA (2002) 3823–3828.

[24] O. C. Zienkiewicz, K. Morgan, Finite Elements and Approximation, Wiley, New York, 1983.

Post-print version of the article: A. Steinboeck, D. Wild, T. Kiefer, and A. Kugi, "A fast simulation method for 1D heat conduction", *Mathematics and Computers in Simulation*, vol. 82, no. 3, pp. 392–403, 2011. DOI: 10.1016/j.matcom.2010.10.016
The content of this post-print version is identical to the published paper but without the publisher's final layout or copy editing.